Carbohydrate Polymers 92 (2013) 157–166

Contents lists available at SciVerse ScienceDirect

Carbohydrate Polymers

journal homepage: www.elsevier.com/locate/carbpol

Preparation and characterization of hydrogels based on homopolymeric fractions of sodium alginate and PNIPAAm

David Leal[a], Wim De Borggraeve[b], Maria V. Encinas[a], Betty Matsuhiro[a,*], Robert Müller[c]

[a] Department of Environmental Chemistry, Faculty of Chemistry and Biology, Universidad de Santiago de Chile, Av. B. O'Higgins 3363, Santiago, Chile
[b] Molecular Design and Synthesis, Department of Chemistry, KU Leuven, Celestijnenlaan 200F, bus 2404, 3001 Heverlee, Belgium
[c] Imec, Polymer and Molecular Electronics, Kapeldreef 75, B-3001 Leuven, Belgium

ARTICLE INFO

Article history:
Received 16 May 2012
Received in revised form 9 August 2012
Accepted 15 September 2012
Available online 24 September 2012

Keywords:
Sodium alginate
Homopolymeric fractions
PNIPAAm
Hydrogels
SEM

ABSTRACT

Graft copolymers were prepared by formation of an amide bond between poly-α-L-guluronic acid (MW 24,000), isolated from sodium alginate and the free amino group of PNIPAAm-NH_2. SEM micrographs revealed the formation of a macroscopic network on the surface of the grafted hydrogels with a porosity diameter of 10–20 μm. Semi-IPN hydrogels were prepared using different proportions of sodium poly-β-D-mannuronate (MW 21,000), isolated from sodium alginate and cross-linked PNIPAAm-NH_2 polymers. SEM micrographs showed porosities of minor size (~5 μm). Though both types of hydrogels are good water containers, the water retention capacity of graft copolymers is more than 50% higher than that of semi-IPN hydrogels. Both hydrogel types showed significant changes in swelling ratios between 20 and 45 °C: the swelling ratio decreases near the LCST of PNIPAAm. The water absorption and retention capacity of graft hydrogels increases with pH, reaching a maximum value at pH 7.0.

1. Introduction

Alginic acid is the major structural polysaccharide of brown seaweeds; it is a linear copolymer of 1→4 linked β-D-mannopyranuronic acid (M) and α-L-gulopyranuronic acid (G). These two uronic acids can be arranged in heteropolymeric (MG) and homopolymeric (MM and GG) blocks (Chandía, Matsuhiro, & Vásquez, 2001; Chandía, Matsuhiro, Mejias, & Moenne, 2004; Leal, Matsuhiro, Rossi, & Caruso, 2008; Painter, 1983). Alginate salts are widely used in pharmaceutical and food industry; they show medical applications in wound dressing, as scaffolds, and as delivery matrices (Donati & Paoletti, 2009; Draget & Taylor, 2011; Draget et al., 2005; Han, Guenier, Salmieri, & Lacroix, 2008; Shapiro & Cohen, 1997; Wang, Liu, Gao, Liu, & Tong, 2008). The cooperative binding of divalent cations (usually Ca^{2+}) between the homopolymeric sequence of G residues gives rise to the gelling properties of alginates (Grant, Morris, Rees, Smith, & Thom, 1973). Semi-interpenetrating hydrogels (semi-IPN) of biodegradable polymers obtained from natural resources with non-toxic synthetic polymers have potential applications because they can combine high responsiveness to an external stimulus with good biocompatibility (Dumitriu, Vidal, & Chornet, 1996; Hoare & Kohane, 2008). De Moura et al. (2005, 2006, 2009) prepared calcium alginate and PNIPAAm interpenetrated hydrogels with potential biomedical applications. Poly(*N*-isopropylacrylamide) (PNIPAAm) is a temperature-sensitive polymer with many applications in medicine and pharmacology (Guo & Gao, 2007; Shi, Alves, & Mano, 2007; Yoo, Seok, & Sung, 2004; Zhang & Peppas, 2002). In the last two decades, also copolymerization of polysaccharides with vinyl polymers (graft hydrogels) has gained much attention since stimuli-responsive hydrogels with novel properties can be prepared in this way (Jenkins & Hudson, 2001; Krishnamoorthi, Mal, & Singh, 2007; Li, Wu, & Liu, 2008; Prabaharan & Mano, 2006; Sanlı, Ay, & Isıklan, 2007).

Synthesis and characterization of graft and semi-IPN hydrogels of commercial sodium alginate with PNIPAAm have been published (Ju, Kim, Kim, & Lee, 2002; Kim, Lee, Kim, & Lee, 2002; Zhang, Zha, Zhou, Ma, & Liang, 2005a, 2005b). In these publications, the authors used commercial alginates with a M/G ratio of 1.56, which indicated an alginate enriched in mannuronic acid; however the composition in terms of hetero- and homopolymeric blocks was unknown. It is important to know the extent of the homopolyguluronic acid block fraction in the polymer since this fraction is responsible for gel formation in the presence of calcium ions. Thus, the use of homo-polymeric blocks obtained from sodium alginate would allow the preparation of hydrogels with characteristic and defined properties. In previous

* Corresponding author at: Facultad de Química y Biología, Casilla 40, Correo 33, Santiago, Chile.
E-mail address: betty.matsuhiro@usach.cl (B. Matsuhiro).

0144-8617/$ – see front matter © 2012 Elsevier Ltd. All rights reserved.
http://dx.doi.org/10.1016/j.carbpol.2012.09.031

work, we performed the isolation of homopolymeric blocks of sodium alginate from the hybrid brown seaweed *Lessonia-Macrocystis*. Full characterisation of these homopolymers was done by vibrational spectroscopy methods along with computational calculations (Cardenas-Jiron, Leal, Matsuhiro, & Osorio-Roman, 2011). The aim of the present work is to synthesize and characterize graft and semi-IPN cross-linked hydrogels bearing a homopolymer block of sodium alginate and poly(*N*-isopropylacrylamide) with an amine group at the end of the polymer chain (PNIPAAm-NH_2). Graft hydrogels were synthesized by covalently linking this amine group to poly-α-L-gulopyranuronic acid blocks (GG) in the presence of Ca^{2+} ions, meanwhile semi-IPN hydrogels were obtained by the association of the cross-linked PNIPAAm chains with poly-β-D-mannopyranuronic acid blocks (MM).

2. Materials and methods

2.1. Materials

Poly-β-D-mannuronic acid (MM) and poly-α-L-guluronic acid (GG) blocks were previously obtained by partial hydrolysis of sodium alginate from the hybrid brown seaweed *Lessonia-Macrocystis* (*LMH*) collected in Tekenika Bay (55°19′60″S, 68°25′0″W), southern Chile (Cardenas-Jiron et al., 2011). *N*-Isopropylacrylamide (NIPAAm) (Sigma–Aldrich Co., St. Louis, MO, USA) was purified by recrystallization from n-hexane/toluene (Merck, Darmstadt, Germany). 2-Aminoethanethiol (AESH), 1-ethyl-(3-3-dimethylaminopropyl) carbodiimide hydrochloride (EDC), *N*-hydroxysuccinimide (NHS) and *N*,*N*′-methylenebisacrylamide (MBA) were purchased from Sigma–Aldrich Co. (St. Louis, MO, USA). Calcium chloride ($CaCl_2$) was purchased from Merck (Darmstadt, Germany). 2,2′-azobisisobutyronitrile (AIBN) (Sigma–Aldrich Co., St. Louis, MO, USA) was recrystallized from methanol (Merck, Darmstadt, Germany). Distilled water was purified using a Milli-Q Barnstead Easypure II system (Thermo Scientific, Dubuque, IA, USA). Tetrahydrofuran (THF), ethyl ether and acetonitrile (ACN) (Merck, Darmstadt, Germany) were of spectroscopic grade and they were used without any further purification.

2.2. Synthesis and molecular weight determination of linear and cross-linked poly(N-isopropyl-acrylamide)

Free radical polymerizations of *N*-isopropylacrylamide were carried out in ACN solution under N_2 gas atmosphere at 25 °C, using AIBN as photoinitiator. AESH was used as chain transfer agent. The samples were irradiated in a Rayonet photochemical reactor (Hamden, CT, USA) equipped with a 360 nm irradiation source. Irradiation times were fixed to obtain conversions <50%. The *N*-isopropylacrylamide concentration was kept constant at 0.6 M, the AIBN concentration was 0.01 M. The polymers were isolated from the low molecular weight compounds by successive precipitations in ethyl ether.

Along with this, cross-linked poly(*N*-isopropylacrylamide) was synthesized under the same previous conditions and by adding 2 wt% MBA, based on the total amount of monomer used in the polymerization. In both cases, the irradiated solutions were dialyzed against distilled water using MWCO 3500 Spectra/Por membrane (Spectrum Laboratories, Inc., Rancho Dominguez, CA, USA) and then precipitated with ten times their volume in cold ethyl ether and washed several times with excess of cold ethyl ether. Finally, the precipitate was dried in vacuum during 24 h at room temperature.

Average molecular weights (M_n) of the synthesized polymers were determined by gel permeation chromatography (GPC) at 25 °C, using an HP 1100 (Hewlett-Packard, Palo Alto, CA, USA) liquid chromatograph, equipped with three series of Styragel HR 1-2-4 (Waters Co., Framingham, MA, USA) columns and THF as mobile phase with a flow rate of 1 mL min^{-1}. Differential refractometry was used to detect the polymers, and monodisperse poly(methyl methacrylate) polymers (PMMA standard, Waters Co., Framingham, MA, USA) were employed for calibration (Zhang et al., 2005a).

2.3. Preparation of GG-g-PNIPAAm graft hydrogels

The sodium salt of poly-α-L-guluronic acid (fraction GG), and linear PNIPAAm-NH_2 bearing the terminal amino group were dissolved in water (2 wt%) at room temperature. EDC and NHS were added to link the polymer chains. The solution had a GG:PNIPAAm weight ratio of 1:1, and a GG:EDC:NHS molar ratio of 2:2:1 with reference to the GG carboxyl group. The mixed solution was continuously stirred overnight at room temperature, and then it was extracted with five times its volume THF–hexane solution (4:1). The aqueous layer was concentrated in vacuo, dialyzed for 48 h in distilled water, and freeze-dried (Freezone 4.5, Labconco Co., Kansas City, MO, USA). Nitrogen content was determined in a CE-440 elemental analyzer (Exeter Analytical, Inc., North Chelmsford, MA, USA).

2.4. Preparation of MM/PNIPAAm semi-IPN hydrogels

The aqueous solution of the sodium salt of poly-β-D-mannuronic acid, MM (5 wt%), and cross-linked PNIPAAm (20 wt%) were mixed in various concentrations (80/20, 50/50 and 20/80 by weight). The mixed solution was poured into a Petri dish and dried to constant weight at room temperature in a vacuum oven.

2.5. IR and NMR spectroscopy

FT-IR spectra of the samples in thin film were registered in the 4000–400 cm^{-1} region using a Bruker IFS 66*v* instrument. Derivation including the Savitzky–Golay algorithm with 23 smoothing points was performed using the OPUS/IR v.1.44 software incorporated into the hardware of the instrument (Leal et al., 2008). ^1H NMR (400.13 MHz) and ^{13}C (100.62 MHz) spectra were recorded at 60 °C in D_2O on a Bruker Avance DRX400 spectrometer after isotopic exchange with D_2O (3× 0.70 mL), using the sodium salt of 3-(trimethylsilyl)propionic 2,2,3,3-d_4 acid as standard. NMR spectra of hydrogels were recorded at 25 °C on a Bruker AvanceII 600 spectrometer equipped with a z-gradient inverse broad band probe of 5 mm diameter, operating at 600.13 MHz (^1H NMR) and 150.90 MHz (^{13}C NMR). All two-dimensional experiments were acquired using a pulse field gradient incorporated into NMR pulse sequences. The two-dimensional homonuclear ^1H–^1H correlation spectroscopy (COSY) was acquired with 128 × 2048 data points having a spectral width of 1200 Hz and processed in a 1024 × 1024 matrix to give a final resolution close to 2.3 Hz $point^{-1}$ in the two-dimensions. The two-dimensional heteronuclear single quantum coherence correlation (2D ^1H–^{13}C HSQC) spectra were acquired with 128 × 2040 data points and processed in a 1024 × 1024 matrix to give a final resolution close to 2.3 Hz $point^{-1}$ in ^1H NMR and close to 2.4 Hz $point^{-1}$ in ^{13}C NMR. The number of scans (ns) in each experiment was dependent on the sample concentrations.

2.6. SEM

The surface morphology of hydrogels was studied by field emission scanning electron microscopy (SEM), using Philips XL 30S FEG equipment (Amsterdam, The Netherlands) with an operating voltage of 5 kV. Samples of graft and semi-IPN hydrogels (0.1 wt%) were dissolved in distilled water at room temperature, quickly frozen in liquid nitrogen and then lyophilized (BenchTop SLC, VirTis, New

Table 1
Polymerization conditions, and average molecular weight M_n (g/mol) of linear poly(*N*-isopropylacrylamide)-NH_2.

Polymer[a]	AESH (mM)	M_n (g/mol)[b]
P-1	0.0	35,700
P-2	9.1	31,000
P-3	18.1	9300
P-4	20.0	9000
P-5	20.0	8900

[a] Poly(*N*-isopropylacrylamide-NH_2).
[b] The average molecular weight was determined by GPC using monodisperse poly(methylmethacrylate) with M_n from 1580 to 52,500 g/mol.

York, NY, USA) for 48 h. The freeze-dried hydrogels were fixed on brass holders and coated by sputtering with a thin Au layer in order to avoid charging effects.

2.7. Swelling properties and stimuli response of hydrogels

To measure the swelling ratio, pre-weighed dry samples were immersed in a $CaCl_2$ solution (0.1 M) at room temperature (25 °C). After removing the water excess on the sample surface using a filter paper, the weight of the swollen samples was measured at different times. The swelling ratio was monitored until there was no considerable change in weight of the hydrogel samples. In addition, the swelling ratios of the hydrogel samples were measured in the temperature range from 20 to 45 °C (at pH 5.4) and in the pH range from 2.0 to 7.0 (at 25 °C) using the gravimetric method described above and the same medium conditions. Under each particular condition, hydrogel samples were incubated in the medium for at least 24 h and weighed after removing the water excess from the samples with filter paper. Each swelling ratio was calculated using the equation:

$$\text{Swelling ratio} = \frac{W_s - W_d}{W_d} \quad (1)$$

where W_s is the weight of hydrogel in the swollen state at a particular condition (time, pH or temperature), and W_d is the dry weight of the hydrogel.

3. Results and discussions

3.1. Synthesis of linear and cross-linked poly(N-isopropylacrylamide)

The molecular weight of PNIPAAm polymers was regulated using different concentrations of chain transfer agent, AESH. It was found that the optimal conditions for the polymerization reaction were a non-protic polar solvent like acetonitrile, the thiol (AESH) concentration around 20 mM, and a low monomer concentration. Under these conditions, polymers with an amine terminal group at the end of polymer chain and a molecular weight in the same order as the homopolymeric fractions (MM and GG) isolated from sodium alginate of *LMH* could be obtained (Cardenas-Jiron et al., 2011). Table 1 shows the molecular weights of various synthesized linear PNIPAAm polymers obtained by GPC. It can be pointed out that the average molecular weight of the polymers decreases markedly with the increase in the AESH concentration as expected from the high efficiencies of aliphatic thiols as chain transfer agents (Valdebenito & Encinas, 2010). The synthesized PNIPAAm-NH_2 polymers were characterized by infrared (FT-IR) and NMR spectroscopies. Fig. 1a shows the FT-IR spectrum of the P-3 polymer, it presents the characteristic bands at 3436.8, 3314.6 and 2929.8 cm^{-1} assigned to primary amino (νN—H), amide (νN—H) and alkane (νC—H) groups, respectively, along with two bands at 1654.0 cm^{-1} and 1544.00 cm^{-1} assigned to amide I (νC═O) and amide II (νN—H), vibrations, respectively (Conley, 1966). Fig. 2a and b shows, respectively, the ^1H and ^{13}C NMR spectra in D_2O of the synthesized PNIPAAm-NH_2 polymer P-3.The ^1H NMR spectrum exhibited a broad signal at 3.82 ppm which was assigned to the H—C proton of the isopropyl group linked to the amide function (—CH—NH—); the broadening of the signal is probably due to a quadrupolar effect of the neighbor nitrogen atom (Hesse, Meier, & Zeeh, 1997). The broad and low intensity signals at 1.94 and 1.51 ppm correspond to the methine and methylene protons, respectively, and the intense signal at 1.07 ppm was assigned to the six methyl protons of the isopropyl group. The chemical shifts of these signals are indicative for the transformation of the vinyl bond in *N*-isopropylacrylamide residues; furthermore, the absence of signals between 5.0 and 6.0 ppm indicates the absence of vinyl monomer in the dialyzed samples. In addition, the ^{13}C NMR spectrum shows a signal at 175.66 ppm that corresponds to the carbonyl carbon (C═O) of the amide groups along with three more signals at 42.20, 35.16 and 22.07 ppm assigned to the methine and methylene carbons (—CH_2—CH<) of the regular polymer chain, and to the methine carbon (—CH—NH—) of the isopropyl group, respectively. No unsaturated carbon signals were observed indicating the absence of monomer molecules.

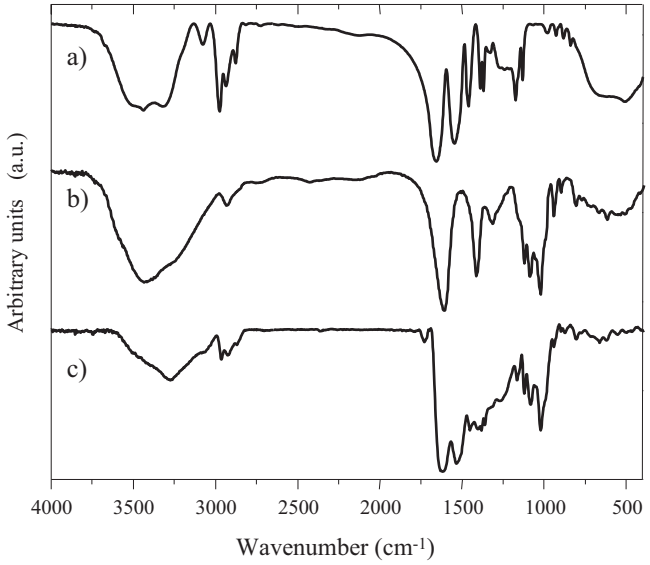

Fig. 1. FT-IR spectra in the 4000–400 cm^{-1} region of: (a) P-3 PNIPAAm-NH_2 (film), (b) sodium poly-α-L-guluronate (in KBr), (c) HGG-2 graft hydrogel (film).

Cross-linked PNIPAAm polymers were synthesized using *N*-*N*′-methylenebisacrylamide (MBA) at 2% (w/w) as cross-linker monomer in the free radical polymerization. These polymers were characterized by ^1H NMR spectroscopy. Fig. 2c presents the ^1H NMR spectrum of a cross-linked polymer of PNIPAAm, it shows a similar profile to that obtained for linear chains. Furthermore, two low intensity peaks between 2.85 and 2.50 ppm could be observed; these signals are assigned to protons of the ethylene group (—CH_2—CH_2—) from the chain transfer agent (AESH) (Kim et al., 2002) as shown in the insert. Along with this, Fig. 2d shows the ^1H NMR spectrum of the PNIPAAm polymer P-1 synthesized without chain transfer agent. No proton signals between 2.85 and 2.50 ppm could be observed, indicating the absence of chain transfer agent inside the polymer structure.

3.2. Synthesis of graft copolymer, GG-g-PNIPAAm

A comb-type hydrogel was prepared by formation of an amide bond between the carboxyl group of poly-L-guluronic acid (MW

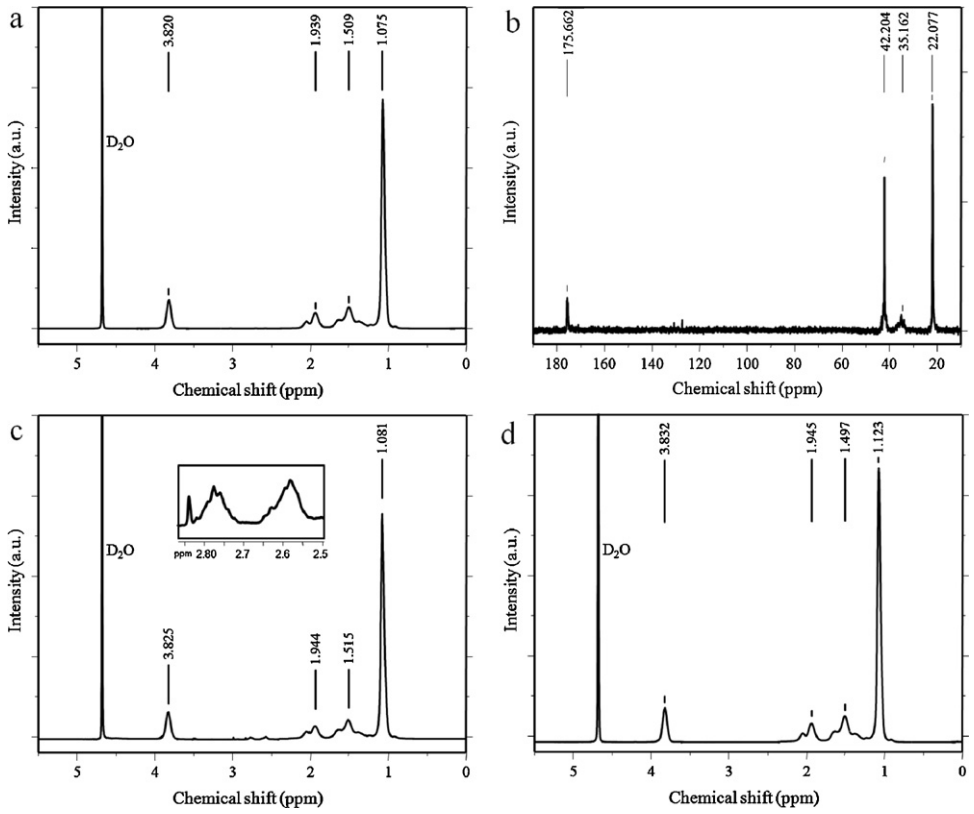

Fig. 2. NMR spectra of synthesized polymers of PNIPAAm in D_2O and 25 °C. (a) ^1H NMR spectrum (400 MHz) of P-3 of linear PNIPAAm-NH_2. (b) ^{13}C NMR spectrum (100 MHz) of P-3 of linear PNIPAAm-NH_2. (c) ^1H NMR spectrum (400 MHz) of cross-linked PNIPAAm-NH_2 using MBA. (d) ^1H NMR spectrum (400 MHz) of linear PNIPAAm (P-1) without chain transfer agent.

24,000) and the free amino group of samples P-3 to P-5 of PNIPAAm-NH_2 using EDC to activate the carboxyl group in the polysaccharide as shown in Scheme 1. The reactive amounts employed during the synthesis are listed in Table 2. It can be pointed out that the reactive amounts used in Table 2 were calculated on basis of the carboxylate groups present in the polysaccharide using the molecular weight of it and the initial mass. Thus, NHS was used as the limiting reagent in order to obtain a certain conjugation percentage of polymer chains into the polysaccharide (Table 2). In addition, elemental analysis of nitrogen was used to determine the actual reaction composition as shown in Table 2. An increase on the nitrogen content can be observed according with the

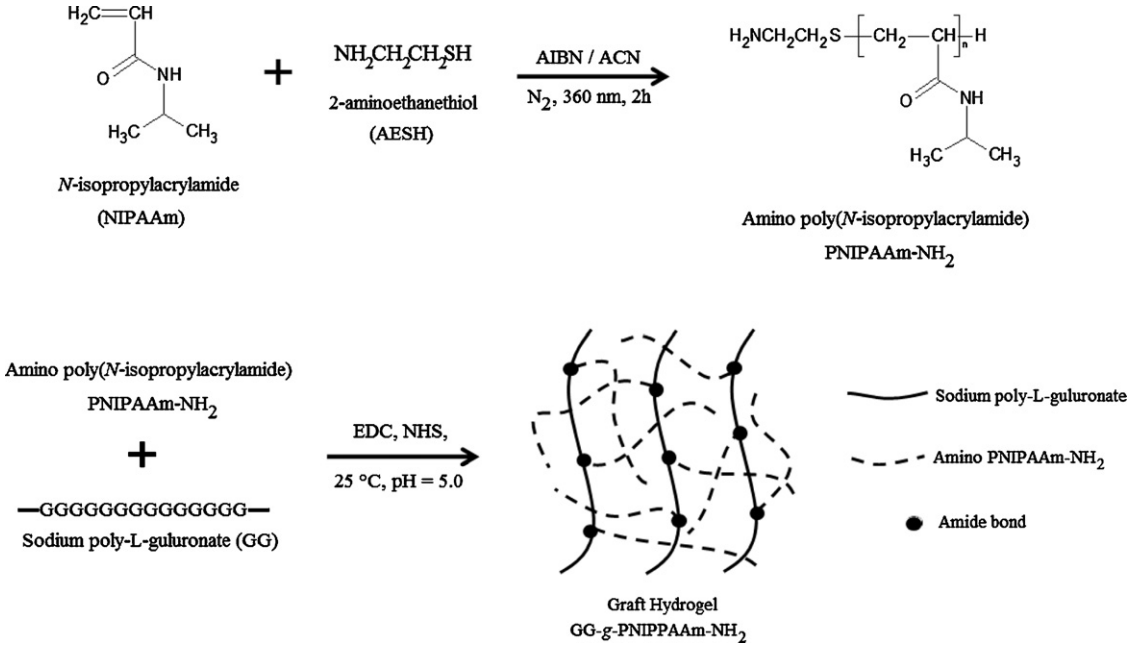

Scheme 1. Formation of graft copolymer of GG and linear PNIPAAm-NH_2.

Table 2
Reactive amounts of poly-α-L-guluronic acid fraction and linear semi-telechelic PNIPAAm-NH_2 in the formation of graft copolymers.

Hydrogel	GG[a] (mg)	EDC[b] (mg)	NHS[c] (mg)	Polymer (mg)	Recovery mass[d] (mg)	N content (wt%)
HGG-1	100	97	15	100	110	1.34
HGG-2	100	97	29	100	116	2.50
HGG-3	100	97	44	100	152	3.35

[a] Homopolymeric blocks of the sodium salt of poly-α-L-guluronic acid.
[b] 1-Ethyl-(3-3-dimethylaminopropyl) carbodiimide hydrochloride.
[c] *N*-Hydroxysuccinimide.
[d] Of the hydrogel.

reaction conditions, indicating the increase on the conjugation level and the introduction of PNIPPAAm-NH_2 on the gel structure. These results are in agreement with those reported by Ju, Kim, and Lee (2001) for alginic acid hydrogels conjugated to PNIPAAm polymers. Three different grafted copolymers were obtained and characterized by spectroscopic methods. Fig. 1b shows the IR spectrum of the sodium salt of polyguluronic acid, obtained by partial depolymerization of sodium alginate, which presents characteristic bands at 3427.5 cm^{-1} (νO—H), 2930.7 cm^{-1} (νC—H), 1614 cm^{-1} (νC═O of carboxylate group), and at 816.67 cm^{-1} assigned to C—O—H ring and C—H of α-anomeric linkage vibrations (Chandía et al., 2001; Leal et al., 2008). The IR spectrum (Fig. 1c) of the graft polymer shows signals at 3276.6 cm^{-1} (νN—H, amide), 2923.6 cm^{-1} (νC—H), 1623.4 cm^{-1} (νC═O, amide I and carboxylate), 1537.2 cm^{-1} (N—H, amide II), and at 809.7 cm^{-1} assigned to C—O—H ring and C—H of α-anomeric linkage vibrations.

Fig. 3 shows the ^{13}C NMR spectrum of HGG-2 graft copolymer. In the carbonyl region (170–180 ppm) it is possible to distinguish at least three carbon peaks, two of them assigned to the carbonyl carbon atoms of the amide group of PNIPAAm-NH_2 (174.25 ppm) and of the carboxylic group of poly-α-L-guluronate (175.65 ppm), the third one due to the amide group formed in the conjugation, at 174.92 ppm. Moreover, the characteristic signals between 102 and 65 ppm assigned to poly-α-L-guluronic acid (Matsuhiro, Torres, & Guerrero, 2007; Leal et al., 2008) and between 43 and 22 ppm assigned to PNIPAAm-NH_2 chains are found. Two-dimensional NMR spectra were registered to confirm the fine structure of the grafted copolymer hydrogels, and assignments of the ^{13}C and ^{1}H NMR spectra were accomplished as shown in Fig. 3.

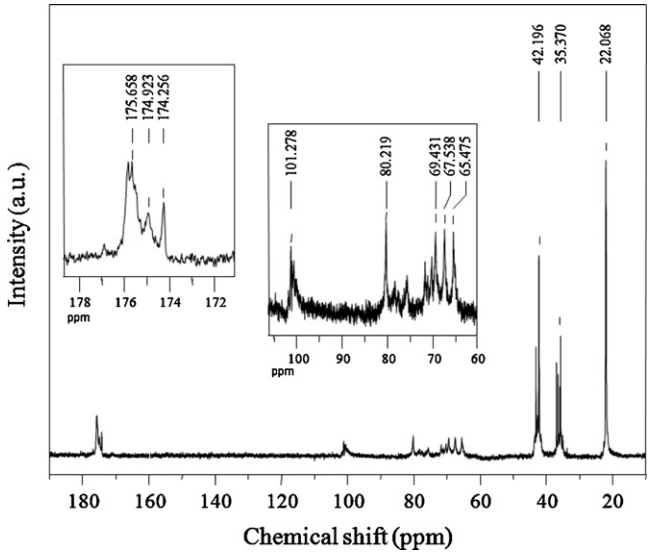

Fig. 3. ^{13}C NMR spectrum (150 MHz) at 25 °C of the graft copolymer HGG-2 in D_2O.

3.3. Preparation of semi-interpenetrating mixture of MM blocks with cross-linked PNIPAAm

The semi-IPN hydrogels were prepared using different proportions of homopolymeric blocks of sodium poly-β-D-mannuronate (MW 21,000) and cross-linked PNIPAAm polymers. The pH of the medium was regulated at 4.0 where the amine groups at the end of polymer chain are protonated and the carboxylic groups of the poly-β-D-mannuronate (pK_a, 3.39) are deprotonated as well. This condition allows the electrostatic interactions of the PNIPAAm-NH_2 with the poly-mannuronate chains as shown in Scheme 2. Three semi-IPN hydrogels were obtained with MM/PNIPAAm ratios of 20/80 percent HMM-1 (95 wt% yield), HMM-2 with a 50/50% (90 wt% yield), and HMM-3 with 80/20% ratio (96 wt% yield).

3.4. Morphologic characterization of graft HGG and semi-IPN HMM hydrogels by scanning electron microscopy

The hydrogel samples, the homopolymeric blocks (MM and GG), and the PNIPAAm-NH_2 polymer were analyzed by scanning electron microscopy (SEM) in order to obtain the morphology and superficial profiles. Fig. 4 shows the SEM micrographs of the internal structure of the homopolymeric blocks along with the PNIPAAm-NH_2 polymer. The images at different magnifications correspond to the homopolymeric blocks showing the laminar distribution in both structures. Small folds can be observed at 2000× on the GG sample (Fig. 4 b) which may be assigned to the tertiary structure of the poly-α-L-guluronic acid chains as pleated sheets. Along with this, the laminar distribution observed in the MM sample (Fig. 4c and d) is probably attributed to the tertiary structure of poly-β-D-mannuronic acid chains as extended sheets (Rees & Welsh, 2003). A completely different pattern was found for the synthetic polymer, PNIPAAm-NH_2. The SEM micrographs (Fig. 4e and f) of P-3 of PNIPAAm-NH_2 polymer show a dense surface with a lack of porosity on it. This is indicative for the contribution of weak attraction forces on the interaction between chains leading to a compact structure across the entire analyzed sample. Fig. 5a and b shows the SEM micrographs of the HGG-1 graft hydrogel. The images reveal the formation of a macroscopic network on the sample surface with a porosity diameter of 10–20 μm. This porous pattern is observed in the rest of the synthesized grafted hydrogels as shown in Fig. 5c and d from HGG-2 and is not observed in the SEM micrographs of each hydrogel component (Fig. 4). According to literature, a hydrophilic dipole is generated between the non-functionalized carboxylic groups of the polysaccharide with the amide groups present in the synthetic polymer which allow the interaction of aqueous solutions and the inside of the hydrogel polymer network (Prabaharan & Mano, 2006). Fig. 5e and f shows the SEM micrographs of HGG-2 cross-linked hydrogel with Ca^{2+} ions. The porous regularity along the structure is due to the arrangement of the polysaccharide chains around the Ca^{2+} ions, forming the "eggs box" structure (Grant et al., 1973). It can be pointed out that the pore formation on the graft hydrogel surface depends on the interaction of the polysaccharide chains with the PNIPAAm-NH_2 polymers

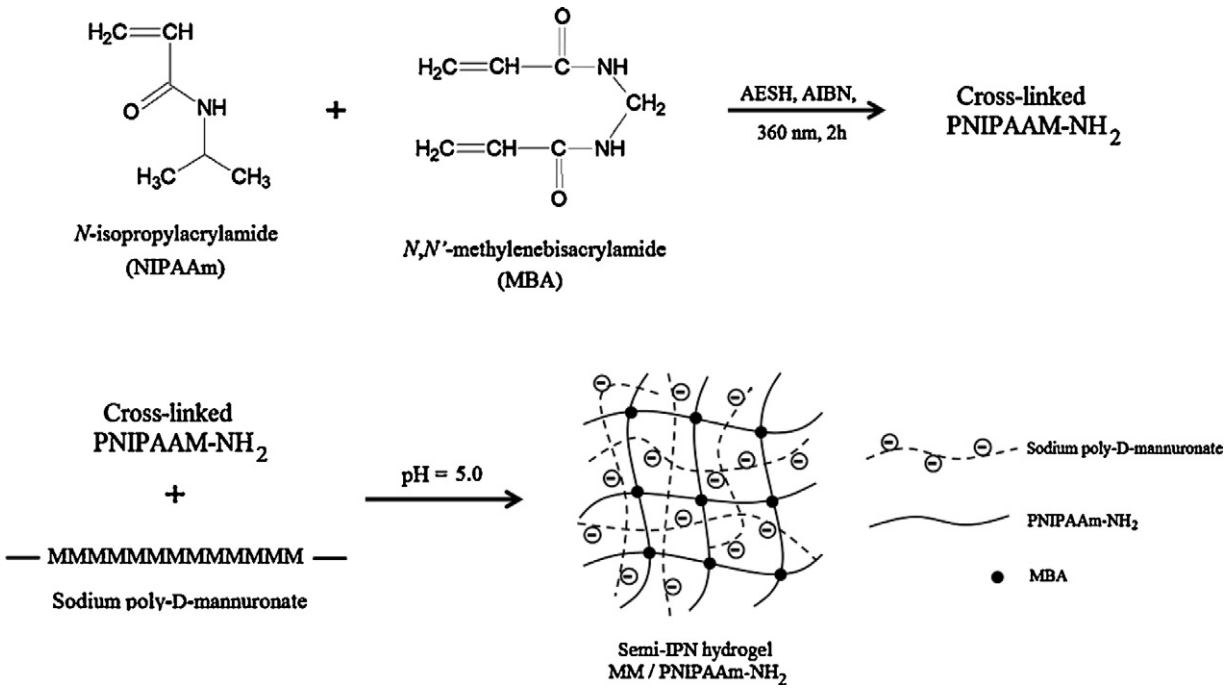

Scheme 2. Formation of semi-IPN hydrogel of MM and cross-linked PNIPAAm-NH_2.

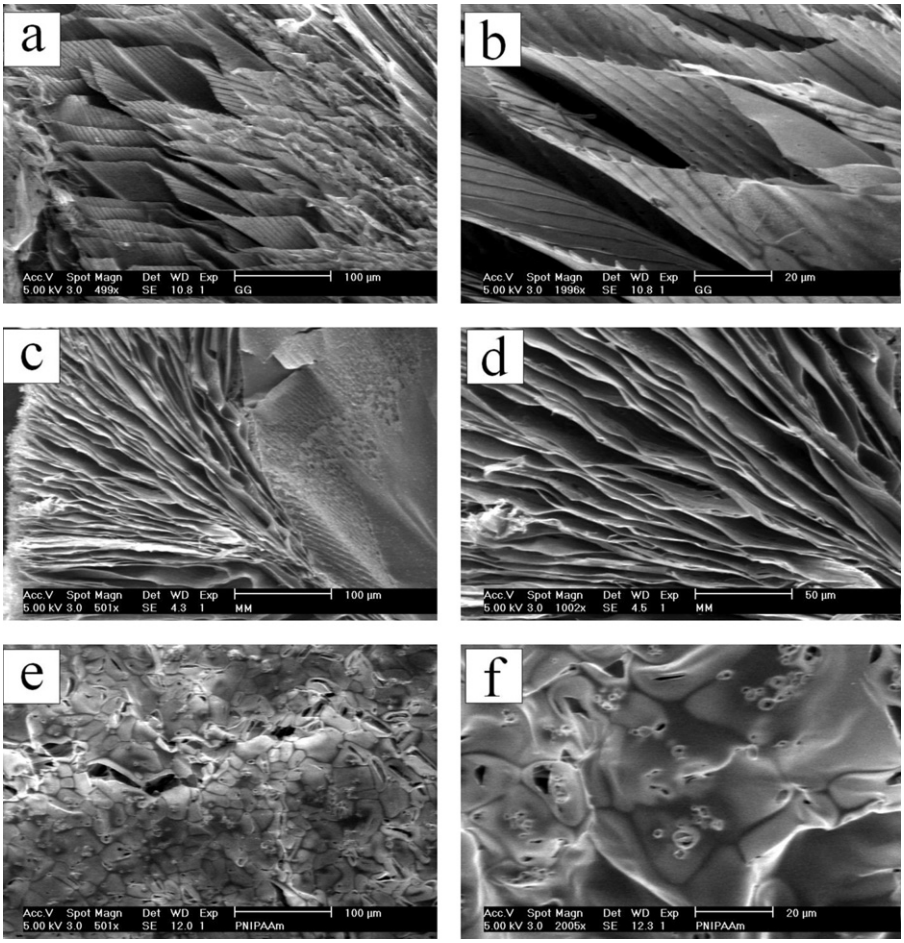

Fig. 4. SEM micrographs of the homopolymeric blocks (MM and GG) and semi-telechelic PNIPAAm-NH_2 polymer: (a) GG at 500×, (b) GG at 2000×, (c) MM at 500×, (d) MM at 1000×, (e) PNIPAAm-NH_2 at 500×, and (f) PNIPAAm-NH_2 at 2000×.

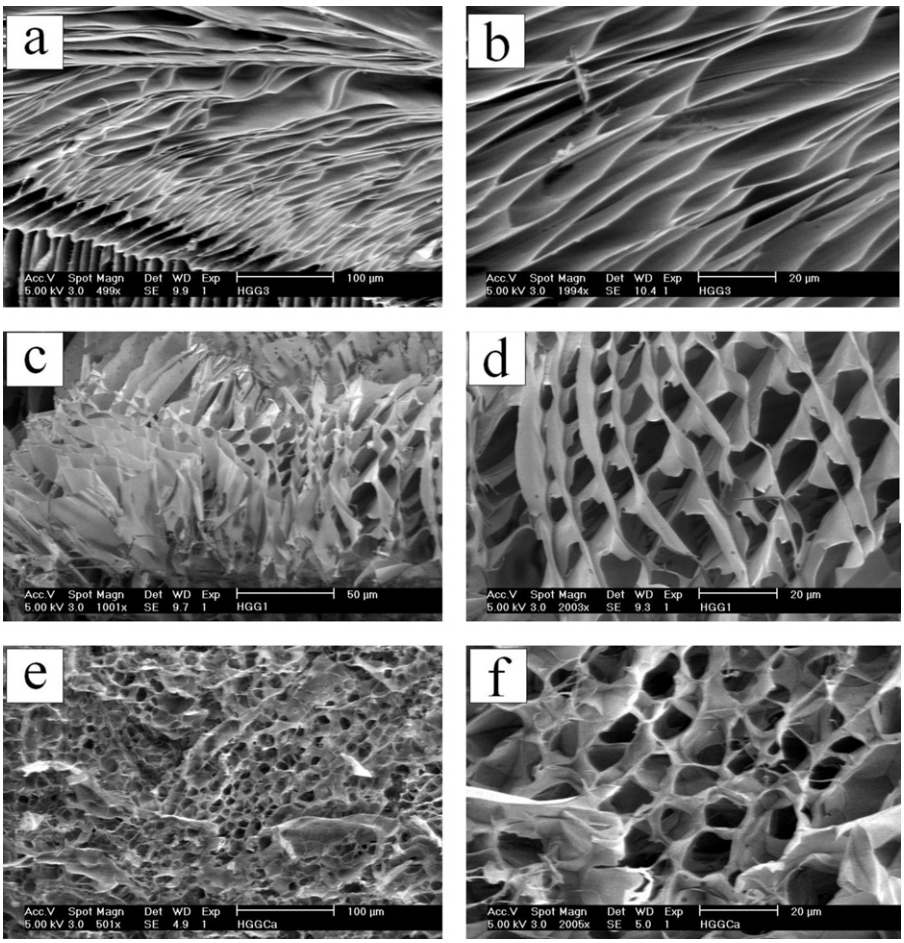

Fig. 5. SEM micrographs of graft hydrogels HGG-1, and HGG-2 along with the HGG-2 cross-linked with Ca^{2+} ions (HGG-2-Ca): (a) HGG-1 at 500×, (b) HGG-1 at 2000×, (c) HGG-2 at 1000×, (d) HGG-2 at 2000×, (e) HGG-2-Ca at 500×, and (f) HGG-2-Ca at 2000×.

as shown in Fig. 5d. Calcium ions allow a better distribution of the polysaccharide chains resulting in an improvement in the pore regularity across the sample. In agreement with the morphologic analysis of the grafted hydrogels, the most regular arrangement observed corresponds to HGG-2 hydrogel (Fig. 5d). Fig. 6 shows the SEM micrographs of semi-IPM hydrogels HMM-2 (Fig. 6a and b) and HMM-1 (Fig. 6c and d). The pore distribution in these hydrogels varies with respect to the graft hydrogels. The electrostatic

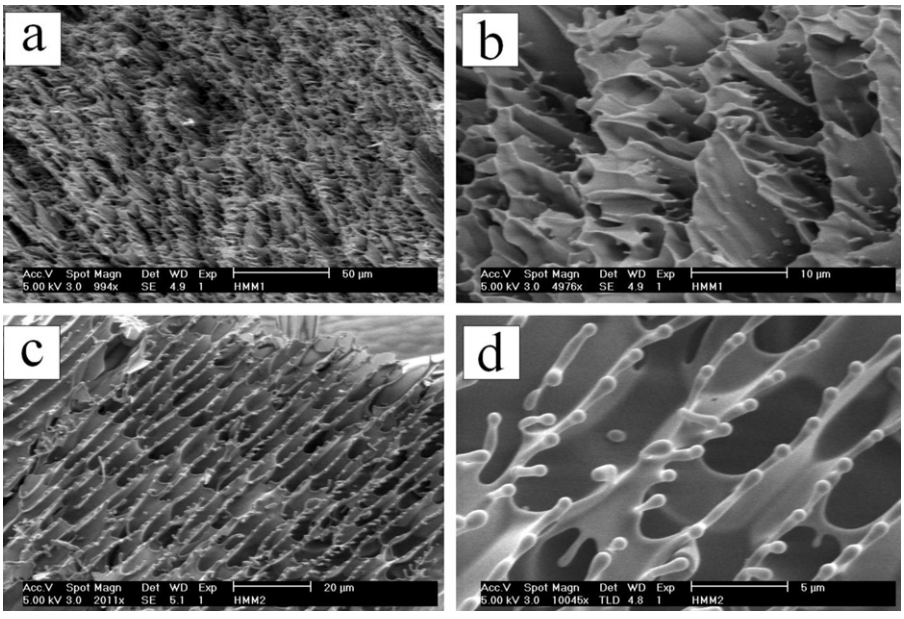

Fig. 6. SEM micrographs of semi-IPN hydrogels HMM-2, and HMM-1: (a) HMM-2 at 1000×, (b) HMM-2 at 5000×, (c) HMM-1 at 2000×, and (d) HMM-1 at 10,000×.

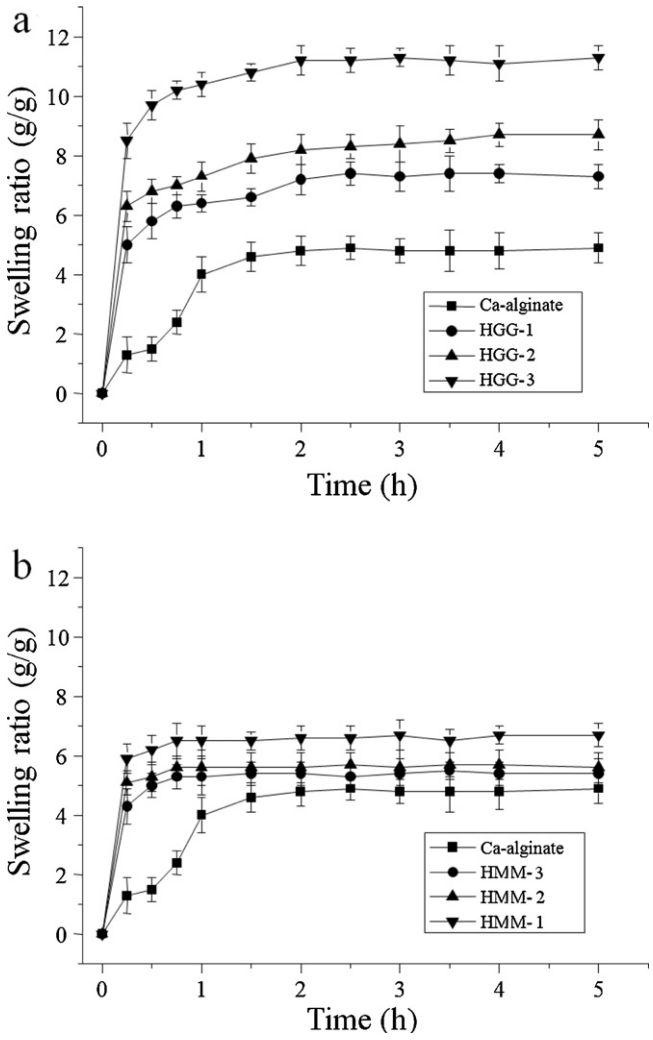

Fig. 7. Swelling kinetics of (a) graft HGG, and (b) semi-IPN HMM hydrogels in a 0.1 M $CaCl_2$ solution at pH = 5.4 and 23 °C.

interaction between the protonated amino groups of PNIPAAm-NH_2 and the carboxylate groups from poly-mannuronate generates pores of reduced size (~5 μm) in comparison to those observed in graft hydrogels. Moreover, "satellite" shapes can be seen surrounding every pore (Fig. 6b and d) which is probably due to the interaction of the polymeric chains of PNIPAAm-NH_2 with the polysaccharide surface. Interestingly, this pattern is observed in all the semi-IPN hydrogels.

3.5. Swelling properties and external stimuli response of graft HGG and semi-IPN HMM hydrogels

The mechanical behavior of the synthesized hydrogels was checked by analyzing their absorption capacity of an aqueous $CaCl_2$ solution over a controlled period of time. The swelling ratio as indicated in Eq. (1) is indicative for this absorption capacity. This ratio is an index of the water absorption capacity along with the increment of the hydrogels volume and the hydrogel resistance in time. In case of graft hydrogels, the formation of the cross-linked network is attributed to the presence of Ca^{2+} ions in the medium. For comparison, alginate microgels were obtained by treatment of native alginate from the hybrid seaweed *Lessonia-Macrocystis* (Cardenas-Jiron et al., 2011) with calcium ions. Fig. 7a shows the swelling ratio of HGG graft hydrogels at 23 °C and pH 5.4, and calcium alginate microgels. The swelling ratio of HGG graft hydrogels increases with the increase of polymer chains bound to the HGG polysaccharide. HGG-3 showed the highest and calcium alginate had the lowest swelling ratio. In addition, these synthesized graft hydrogels showed a remarkable increment in the water retention capacity values compared with reported data for hydrogels of similar characteristics but using commercial sodium alginate (Ju et al., 2001). The swelling ratios of semi-IPN hydrogels (HMM) under the same external conditions are shown in Fig. 7b. Similarly to that described for the graft hydrogels, the incorporation of the synthetic polymers to the network increases the water retention capacity. On the other hand, the water equilibrium inside of the network of the graft hydrogels is reached after 2 h of exposition while the equilibrium in semi-IPN hydrogels is reached after 30–45 min of exposition as shown in Fig. 7b. These results indicate that both microgels, containing the homopolymer blocks, are good water containers with particular features compared with the native polysaccharide. It is noteworthy that calcium alginate showed lower water absorption capacity compared with graft and semi-IPN hydrogels. This is probably due to the polysaccharide arrangement, where the amount of GG blocks is lower than 50% of the composition and the gel formation only depends on the calcium coordination among the alginate chains; this leads to a cross-linked structure but the conjugation (grafting) in HGG hydrogels or the semi interpenetrating network in HMM hydrogels improved on the polymers network swelling. The minor period of time to reach the equilibrium in semi-IPN hydrogels is probably due to the nature of the interactions that predominate within the polymeric network. Since polymeric chains interactions are electrostatic type, between carboxylate groups of the poly-β-D-mannuronate chains and the protonated amine groups of the PNIPPAAm-NH_2 chains, the hydrophilic setting allows a better interaction with aqueous solutions which leads to reach the swelling equilibrium in less time. In contrast, on graft hydrogels, chains from different nature interact between them due to covalent links after the conjugation which reduces the availability of free hydrophilic carboxylate groups to interact with the incoming aqueous solutions. This leads to slower retentions of aqueous solutions inside the polymeric network for graft hydrogels compared with semi-IPN hydrogels. On the other hand, the higher water retention capacity observed in graft hydrogels (Fig. 7a) with respect to semi-IPN hydrogels is probably due to the rigidity of the cross-linked polymer chains of PNIPAAm in these hydrogels. Unlike the cross-linking with calcium ions on the GG chains in graft hydrogels, the covalent cross-linking of PNIPAAm chains in semi-IPN hydrogels restricts the polymeric network expansibility and limits the water retention capacity of the three semi-IPN hydrogels. It can be pointed out that the water retention capacity of semi-IPN hydrogels is more than 50% less compared with graft hydrogels and a remarkable difference among the set of semi-IPN hydrogels it is not observable. In the case of graft hydrogels HGG, the ionic interactions with calcium ions generate greater flexibility and thus increase the retention capacity. Moreover, it can be observed a considerable increment on the retention capacity at higher levels of conjugation despite the higher equilibrium times reached by these hydrogels compared with semi-IPN types. However, the rigidity of HGG hydrogels is affected at higher levels of conjugation; HGG-3 and HGG-2 samples presented a higher flexibility (network expansion) and therefore a more complex handling of the hydrogels "spheres" compared with the most rigid sample, HGG-1. It can be inferred that the conjugation degree is inversely proportional to the stiffness of the synthesized hydrogels. In addition, a possible explanation of the major retention capacity of graft hydrogels can be pointed from the analyzed SEM images. The porous diameters observed in the graft hydrogels (Fig. 5d and f) are bigger than the observed to the semi-IPN samples (Fig. 6b and d). The HGG-2 hydrogel shows a porous diameter close to 10 μm which involves a higher influx of water inside the polymeric network compared to

the semi-IPN HMM-1 hydrogel, whose porous diameter is around 5 μm.

The effect of the temperature and pH on the water retention capacity of graft (HGG) and semi-IPN (HMM) hydrogels was evaluated in order to obtain the swelling ratios behaviors under external stimuli. The swelling equilibrium of HGG and HMM hydrogels as a function of temperature is shown in Fig. 8a and b, respectively. In both figures, the temperature range used was from 20 to 45 °C with increments of 5 °C per sample measurement. Both hydrogels show significant changes in the swelling ratios in all the studied temperature range. The swelling ratio decreases nearby the lower critical solution temperature (LCST) of the PNIPAAm polymers at 32–33 °C. A more drastic change of the capacity of water retention is observed on grafted hydrogels than on semi-IPN hydrogels. At temperature values lower than LCST (20–32 °C), the PNIPAAm polymer chains present expandable and hydrophilic characteristics allowing the water retention capacity. Along with this, hydrophilic interactions due to the presence of free carboxylate groups inside the polymer network in both hydrogel types help on the water retention capacity of these materials. At higher temperatures, close to the LCST of PNIPAAm, the water absorption capacity in both hydrogel types decreases. This effect has been attributed to the collapse of the PNIPAAm chains in the polymer network (De Moura et al., 2005, 2006; Guo & Gao, 2007), and is in agreement with data shown in Fig. 8a and b where the observed changes for the hydrogels with higher content of PNIPAAm, HGG-3 and HMM-1, shows the more pronounced phase transition. At temperatures in the range 40–45 °C the water absorption capacity of HGG-3 and HMM-1 is lower compared to that reported for hydrogels based on alginate with PNIPAAm (Zhao, Cao, Li, Li, & Xu, 2010). This behavior could be explained considering the polysaccharide/polymer ratio, since HGG-3 and HMM-1 present higher amounts of PNIPAAm on the polymer network; in these hydrogels the hydrophilic interactions decrease inside the polymer network and encourage hydrophobic forces that release water outside of the cross-linked polymer network.

Fig. 8c shows the water absorption dependence of graft hydrogels (HGG) with pH changes from 2.0 to 7.0. Hydrogels samples were dissolved in water and then immersed in a $CaCl_2$ solution (0.1 M), and the pH was regulated with a NaOH solution (0.1 M) with increment of 1.0 unit in the pH scale. These results show that the water absorption capacity of graft hydrogels at pH 2.0 is lower than that at pH 5.4. In addition, the water absorption and retention capacity increases at higher pH values with a maximum value at pH 7.0. The water absorption increases with increasing pH values, probably due to the ionic nature inside the hydrogel polymer network. The poly-α-L-guluronate (GG) chains in graft hydrogels have large amounts of carboxylate groups which at acidic pH values are protonated (guluronic acid $pK_a = 3.2$). This allows the generation of hydrophobic points along the polymer network which restrained the entry of water into the network in addition with the increment of the interactions by hydrogen bonds which generate a strengthening and avoiding the network expansion. Thus, hydrogen bond interactions between carboxylic acid groups from polysaccharide and amide groups from the synthetic polymer are increased and then, lead to higher polymer–polysaccharide interactions above polysaccharide–water or polymer–water interactions. Furthermore, charge repulsion among carboxylate groups disappears at acidic pH values which mean that polymer network shrinks and induces the low water absorption at pH < 4.0. Moreover, hydrogels with a lower degree of PNIPAAm conjugated chains (HGG-1 and HGG-2) present lower water absorption capacity than that of HGG-3 hydrogels. This could be explained by the lower carboxylate groups present in HGG-3respect to HGG-1 and HGG-2 graft copolymers. At pH values >4.0, the amount of carboxylate groups increases leading to charge repulsion interactions among these functional

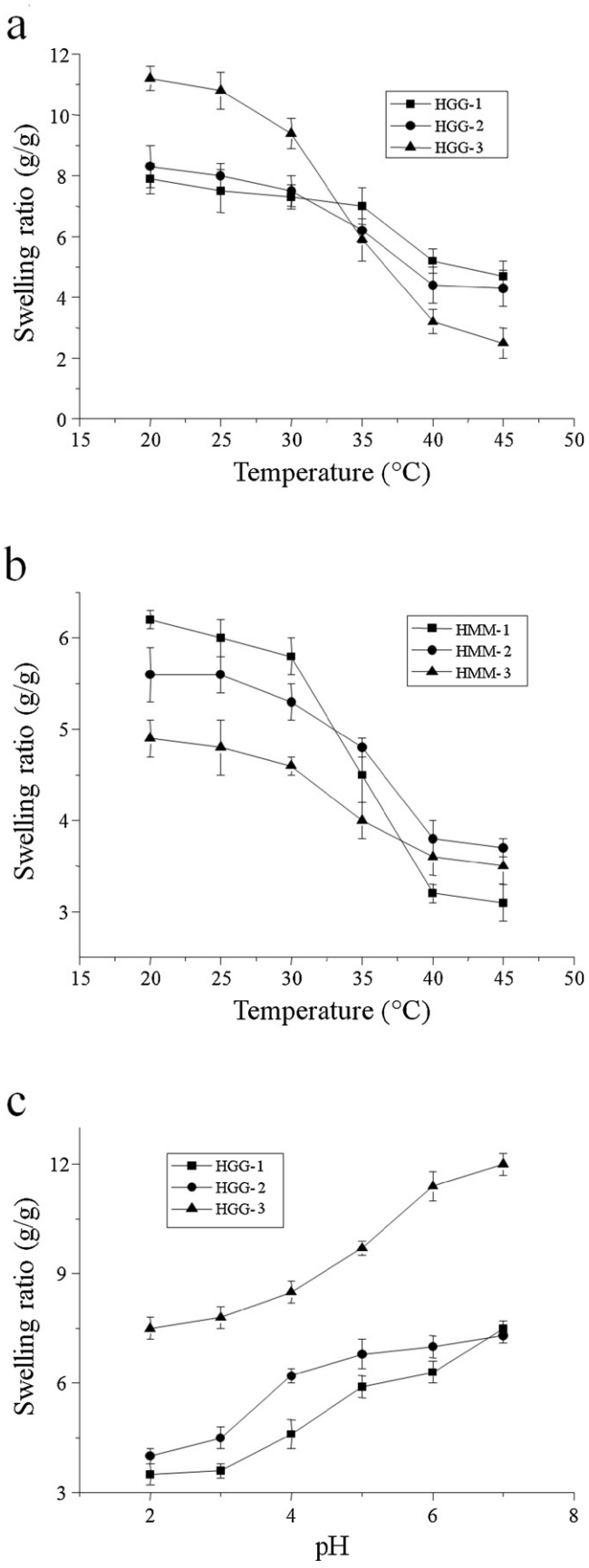

Fig. 8. Swelling ratios as function of temperature and pH of graft and semi-IPN hydrogels. Temperature effect (20–45 °C) in a 0.1 M $CaCl_2$ solution at pH = 5.4 on (a) graft HGG hydrogels, and (b) semi-IPN HMM hydrogels swelling ratios. (c) pH effect (2.0–7.0) in a 0.1 M $CaCl_2$ solution at 25 °C on graft HGG hydrogels swelling ratios.

groups, instead of hydrogen bond interactions. In consequence, the predominance of electrostatic repulsions leads to the network expansion and then, the water absorption capacity increases. The maximum value is reached at pH 7.0.

On the other hand, semi-IPN HMM hydrogels collapsed at pH values between 2.0 and 5.0, probably due to the low electrostatic force exerted by carboxylate groups and protonated amine groups on the polymeric network. At pH 6.0, samples could form compact hydrogels but the highly expansion of the network results in unmanageable materials.

4. Conclusions

A carefully control of the chain transfer agent (AESH) allowed the synthesis of PNIPAAm polymers with well-defined molecular weights.

Graft hydrogels composed of poly-L-guluronate (GG) showed superior water retention capacity over semi-IPN hydrogels under the same external conditions, and also, showed superior water retention capacity than the native sodium alginate. Comb-type (graft HGG) and semi-IPN (HMM) hydrogels exhibited changes in swelling behavior under external stimuli, showing a change in swelling ratio at temperatures higher than 32–33 °C. The most abrupt change in swelling ratio was at 35 °C, nearby the human corporal temperature. Under the influence of pH changes, graft hydrogels showed an increment of their swelling ratios following the pH increase from acidic to neutral media. On the contrary, semi-IPN hydrogel polymer networks collapsed under acidic pH values and are stabilized at neutral pH values.

From the results obtained in this work it can be concluded that copolymers obtained by conjugation of poly-L-guluronate (GG) with PNIPAAm constitute very suitable pH and temperature responsive hydrogels for potential biomedical applications.

Acknowledgements

Financial support of DICYT (Universidad de Santiago de Chile) is gratefully acknowledged. D. Leal was recipient of a doctoral fellowship (D-21080606) and Grant AT-24091086 from CONICYT (Chile); and a fellowship No. UCH-0601 from MECESUP (Chile). The authors thank Dr. M.C. Matulewicz and Dr. T. Barahona (Universidad de Buenos Aires, Argentina) for helpful assistance.

References

Cardenas-Jiron, G., Leal, D., Matsuhiro, B., & Osorio-Roman, I. O. (2011). Vibrational spectroscopy and density functional theory calculations of poly-D-mannuronate and heteropolymeric fractions from sodium alginate. *Journal of Raman Spectroscopy*, *42*, 870–878.

Chandía, N. P., Matsuhiro, B., & Vásquez, A. E. (2001). Alginic acids in *Lessonia trabeculata*: Characterization by formic acid hydrolysis and FT-IR spectroscopy. *Carbohydrate Polymers*, *46*, 81–87.

Chandía, N. P., Matsuhiro, B., Mejias, E., & Moenne, A. (2004). Alginic acid in *Lessonia vadosa*: Partial hydrolysis and elicitor properties of the polymannuronic acid fraction. *Journal of Applied Phycology*, *16*, 127–133.

Conley, R. T. (1966). *Infrared spectroscopy*. Boston: Allyn and Bacon., pp. 157–175.

De Moura, M. R., Guilherme, M. R., Campese, G. M., Radovanovic, E., Rubira, A. F., & Muniz, E. C. (2005). Porous alginate-Ca^{2+} hydrogels interpenetrated with PNIPAAm networks: Interrelationship between compressive stress and pore morphology. *European Polymer Journal*, *41*, 2845–2852.

De Moura, M. R., Aouada, F. A., Guilherme, M. R., Radovanovic, E., Rubira, A. F., & Muniz, E. C. (2006). Thermo-sensitive IPN hydrogels composed of PNIPAAm gels supported on alginate–Ca^{2+} with LCST tailored close to human body temperature. *Polymer Testing*, *25*, 961–969.

De Moura, M. R., Aouda, F. A., Favaro, S. L., Radovanovic, E., Rubira, A. F., & Muniz, E. C. (2009). Release of BSA from porous matrices constituted of alginate–Ca^{2+} and PNIPAAm-interpenetrated networks. *Materials Science and Engineering C*, *29*, 2319–2325.

Donati, I., & Paoletti, S. (2009). In B. H. A. Rehm (Ed.), *Material properties of alginates: Biology and applications* (p. 265). Berlin: Springer-Verlag.

Draget, K. I., & Taylor, C. (2011). Chemical, physical and biological properties of alginates and their biomedical implications. *Food Hydrocolloids*, *25*, 251–256.

Draget, K. I., Smidsrød, O., & Skjåk-Bræk, I. (2005). Alginate from algae. In A. Steinbüchel, & S. K. Rhee (Eds.), *Polysaccharides and polyamides in the food industry. Properties, production, and patents* (p. 30). Weinheim: Wiley-VCH.

Dumitriu, S., Vidal, P., & Chornet, E. (1996). Hydrogels based on polysaccharides. In S. Dumitriu (Ed.), *Polysaccharides in medicinal applications* (pp. 125–262). New York: Marcel Dekker.

Grant, G., Morris, E. R., Rees, D. A., Smith, P. J. C., & Thom, D. (1973). Biological interaction between polysaccharides and divalent cations. The egg-box model. *FEBS Letters*, *32*, 195–198.

Guo, B., & Gao, Q. (2007). Preparation and properties of a pH/temperature-responsive carboxymethyl chitosan/poly(N-isopropylacrylamide)semi-IPN hydrogel for oral delivery of drugs. *Carbohydrate Research*, *342*, 2416–2422.

Han, J., Guenier, A., Salmieri, S., & Lacroix, M. (2008). Alginate and chitosan functionalization for micronutrient encapsulation. *Journal of Agricultural and Food Chemistry*, *56*, 2528–2535.

Hesse, M., Meier, H., & Zeeh, B. (1997). *Spectroscopic methods in organic chemistry*. Stuttgart: Georg Thieme Verlag., pp. 71–72.

Hoare, T. R., & Kohane, D. S. (2008). Hydrogels in drug delivery: Progress and challenges. *Polymer*, *49*, 1993–2007.

Jenkins, D. W., & Hudson, S. M. (2001). Review of vinyl graft copolymerization featuring recent advances toward controlled radical-based reactions and illustrated with chitin/chitosan trunk polymers. *Chemical Review*, *101*, 3245–3273.

Ju, H. K., Kim, S. Y., & Lee, Y. M. (2001). pH/temperature-responsive behaviors of semi-IPN and comb-type graft hydrogels composed of alginate and poly(N-isopropylacrylamide). *Polymer*, *42*, 6851–6857.

Ju, H. K., Kim, S. Y., Kim, S. J., & Lee, Y. M. (2002). pH/temperature-responsive semi-IPN hydrogels composed of alginate and poly(N-isopropylacrylamide). *Journal of Applied Polymer Science*, *97*, 1931–1940.

Kim, J. H., Lee, S. B., Kim, S. J., & Lee, Y. M. (2002). Rapid temperature/pH response of porous alginate-g-poly(N-isopropylacrylamide). *Polymer*, *43*, 7549–7558.

Krishnamoorthi, S., Mal, D., & Singh, R. P. (2007). Characterization of graft copolymer based on polyacrylamide and dextran. *Carbohydrate Polymers*, *69*, 371–377.

Leal, D., Matsuhiro, B., Rossi, M., & Caruso, F. (2008). FT-IR spectra of alginic acid block fractions in three species of brown seaweeds. *Carbohydrate Research*, *343*, 308.

Li, X., Wu, W., & Liu, W. (2008). Synthesis and properties of thermo-responsive guar gum/poly(N-isopropylacrylamide) interpenetrating polymer network hydrogels. *Carbohydrate Polymers*, *71*, 394–402.

Matsuhiro, B., Torres, S., & Guerrero, J. (2007). Block structure in alginic acid from *Lessonia vadosa* (Laminariales, Phaeophyta). *Journal of Chilean Chemical Society*, *52*, 1095–1098.

Painter, T. (1983). Algal polysaccharides. In G. O. Aspinall (Ed.), *The polysaccharides* (pp. 196–285). Orlando: Academic Press.

Prabaharan, M., & Mano, J. F. (2006). Stimuli-responsive hydrogels based on polysaccharides incorporated with thermo-responsive polymers as novel biomaterials. *Macromolecular Bioscience*, *6*, 991–1008.

Rees, D. A., & Welsh, E. J. (2003). Secondary and tertiary structure of polysaccharides. *Angewandte Chemie-International Edition*, *16*, 214–224.

Sanlı, O., Ay, N., & Isıklan, N. (2007). Release characteristics of diclofenac sodium from poly(vinyl alcohol)/sodium alginate and poly(vinyl alcohol)-grafted-poly(acrylamide)/sodium alginate blend beads. *European Journal of Pharmaceutics and Biopharmaceutics*, *65*, 204–214.

Shapiro, L., & Cohen, S. (1997). Novel alginates sponges for cell culture and transplantation. *Biomaterials*, *18*, 563–690.

Shi, J., Alves, N. M., & Mano, J. F. (2007). Thermally responsive biomineralization on biodegradable substrates. *Advanced Functional Materials*, *17*, 3312–3318.

Valdebenito, A., & Encinas, M. V. (2010). Effect of solvent on the free radical polymerization of N,N-dimethylacrylamide. *Polymer International*, *59*, 1246–1251.

Wang, C., Liu, H., Gao, Q., Liu, X., & Tong, Z. (2008). Alginate–calcium carbonate porous microparticle hybrid hydrogels with versatile drug loading capabilities and variable mechanical strengths. *Carbohydrate Polymers*, *71*, 476–480.

Yoo, M. K., Seok, W. K., & Sung, Y. K. (2004). Characterization of stimuli-sensitive polymers for biomedical applications. *Macromolecular Symposia*, *207*, 173–186.

Zhang, J., & Peppas, N. A. (2002). Morphology of poly(methacrylic acid)/poly(N-isopropylacrylamide) interpenetrating polymeric networks. *Journal of Biomaterials Science-Polymer Edition*, *13*, 511–525.

Zhang, G.-Qi, Zha, L.-S., Zhou, M.-H., Ma, J.-H., & Liang, B.-R. (2005a). Preparation and characterization of pH- and temperature-responsive semi-interpenetrating polymer network hydrogels based on linear sodium alginate and cross-linked poly(N-isopropylacrylamide). *Journal of Applied Polymer Science*, *97*, 1931–1940.

Zhang, G.-Qi, Zha, L.-S., Zhou, M.-H., Ma, J.-H., & Liang, B.-R. (2005b). Rapid deswelling of sodium alginate/poly(N-isopropylacrylamide) seminterpenetrating polymer network hydrogels in response to temperature and pH changes. *Colloid and Polymer Science*, *283*, 431–438.

Zhao, S., Cao, M., Li, H., Li, L., & Xu, W. (2010). Synthesis and characterization of thermo-sensitive semi-IPN hydrogels based on poly(ethylene glycol)-co-poly(ε-caprolactone) macromer, N-isopropylacrylamide, and sodium alginate. *Carbohydrate Research*, *345*, 425–431.